NRH:Quinone Oxidoreductase 2 and NAD(P)H:Quinone Oxidoreductase 1 Protect Tumor Suppressor p53 against 20S Proteasomal Degradation Leading to Stabilization and Activation of p53

Xing Gong, Labanyamoy Kole, Karim Iskander, and Anil K. Jaiswal

Department of Pharmacology, Baylor College of Medicine, One Baylor Plaza, Houston, Texas

Abstract

Tumor suppressor p53 is either lost or mutated in several types of cancer. MDM2 interaction with p53 results in ubiquitination and 26S proteasomal degradation of p53. Chronic DNA damage leads to inactivation of MDM2, stabilization of p53, and apoptotic cell death. Here, we present a novel MDM2/ubiquitination-independent mechanism of stabilization and transient activation of p53. The present studies show that 20S proteasomes degrade p53. The 20S degradation of p53 was observed in ubiquitin-efficient and -deficient cells, indicating that this pathway of degradation did not require ubiquitination of p53. The cytosolic quinone oxidoreductases [NRH:quinone oxidoreductase 2 (NQO2) and NAD(P)H:quinone oxidoreductase 1 (NQO1)] interacted with p53 and protected p53 against 20S proteasomal degradation. Further studies revealed that acute exposure to radiation or chemical leads to induction of NQO1 and NQO2 that stabilizes and transiently activates p53 and downstream genes. These results suggest that stress-induced NQO1 and NQO2 transiently stabilize p53, which leads to protection against adverse effects of stressors. [Cancer Res 2007;67(11):5380–8]

Introduction

The p53 protein, called "the guardian of the genome," represents a key regulator of the control of cell growth (1). MDM2 and other E3 ligases interact with p53 that leads to ubiquitination and 26S proteasome–mediated degradation of p53 (2). In response to a variety of stress signals, the p53 protein is stabilized and activated as a sequence specific transcription factor (1). This then leads to cell cycle arrest, senescence, or apoptosis (1).

Quinone oxidoreductases [NAD(P)H:quinone oxidoreductase 1 (NQO1) and NRH:quinone oxidoreductase 2 (NQO2)] are cytosolic proteins that catalyze metabolism of quinones (3, 4). NQO1 and NQO2 are ubiquitously present in all tissues types and induced along with a battery of defensive genes in response to stresses including xenobiotics, antioxidants, oxidants, heavy metals, UV light, and ionizing radiation (5). The coordinated induction of these genes provides necessary protection for cells against free radical damage, oxidative stress, and neoplasia.

NQO1-null and NQO2-null mice were generated (6, 7). These mice were born and developed normal. The studies on NQO1-null and NQO2-null mice revealed altered intracellular redox status and altered metabolism (8). In addition, the studies showed that loss of NQO1 gene expression in NQO1-null mice and NQO2 in NQO2-null mice led to myelogenous hyperplasia of bone marrow and increased sensitivity to skin carcinogenesis in response to benzo(*a*)pyrene and dimethylbenzanthracene (7, 9–12).

Both NQO1-null and NQO2-null mice showed lower basal levels of tumor suppressor protein p53 and decreased apoptosis in skin cells (12, 13). Interestingly, the chemical treatment of skin failed to induce p53 and apoptosis in NQO1-null and NQO2-null mice compared with wild-type mice (12, 13). The lower basal levels and lack of induction of p53 were suggested to have contributed to increased susceptibility of NQO1-null and NQO2-null mice to benzo(*a*)pyrene-induced and dimethylbenzanthracene-induced skin carcinogenesis (12, 13). However, the mechanism of the lower basal level and lack of induction of p53 in NQO1-null and NQO2-null mice remain unknown. Cellular studies showed a role of NQO1 in stabilization of tumor suppressor protein p53 (14). They also revealed that NQO1 stabilizes p53 through a distinct pathway (15), which is independent of MDM2 and ubiquitination (16). In addition, cellular studies reported that NQO1 interacts with p53, and this interaction stabilizes p53 (17). However, the *in vivo* interaction of NQO1 with p53 and its role in p53 regulation and significance of NQO1 regulation of p53 remain unknown. In addition, there is absolutely no information on the role of NQO2 in interaction or regulation of p53.

We used cell and animal (NQO2-null and NQO1-null mice) models to investigate the role of NQO2 and NQO1 in regulation of p53 and significance of this in increased susceptibility to radiation/chemical carcinogenesis. Small interfering RNA (siRNA) inhibition of NQO2 and NQO1 in human hepatoblastoma (Hep-G2) cells showed significant decreases in the levels of p53. This was similar to that observed earlier in NQO2-null and NQO1-null mice. The results also showed that both NQO2 and NQO1 interacted with p53 that led to stabilization of p53. The results further showed that NQO2 and NQO1 suppressed ubiquitin-independent 20S proteasomal degradation of p53 that led to the stabilization of p53. Radiation/chemical exposure of NQO1-expressing and NQO2-expressing mouse keratinocytes led to increase in NQO1 and NQO2 and activation of p53. This activation of p53 was significantly compromised in NQO1-deficient and NQO2-deficient keratinocytes. These results together suggest that exposure to radiation/chemical stress leads to increase in cytosolic NQO2 and NQO1 proteins that interact and protect p53 from 20S proteasome degradation. This leads to stability and transient activation of p53 and cellular protection.

Materials and Methods

Plasmids. The full-length PCR-amplified products of NQO2/NQO1 were separately cloned in pcDNA3.1/V5-HisTOPO vector to generate plasmids

Requests for reprints: Anil K. Jaiswal, Department of Pharmacology, Baylor College of Medicine, One Baylor Plaza, Houston, TX 77030. Phone: 713-798-7691; Fax: 713-798-3145; E-mail: ajaiswal@bcm.tmc.edu.

doi:10.1158/0008-5472.CAN-07-0323

pcDNA-NQO2-V5 and pcDNA-NQO1-V5. A modified polylinker, containing a Kozak start sequence, two Flag epitopes placed adjacent to each other, and stop codons in each frame, was cloned into pCMV vector to generate Flag vector. The NQO2/NQO1 cDNA was cloned at *Xba*I and *Bam*H1 restriction sites at 5′ and 3′ end respectively to generate Flag-NQO2 and Flag-NQO1 expression plasmids. The V5 and Flag plasmids were confirmed by sequencing and expression of V5 or Flag-tagged NQO2 and NQO1 in transfected cells.

Cell culture. Hep-G2 and mouse hepatoma (Hepa-1) cells were cultured in monolayer in MEM and DMEM, respectively, supplemented with 10% fetal bovine serum (FBS), penicillin (40 units/mL), streptomycin (40 μg/mL), and mycostatin (25 μg/mL). The cells were grown at 37°C in 90% air and 10% CO_2. A31N-ts20 is a BALB/c mouse cell line that harbors a temperature-sensitive E1 enzyme, the only ubiquitin-activating enzyme in mammalian cells (18). So that when A31N-ts20 cells are cultured at the restrictive temperature (39°C), the E1 enzyme is inactive and protein ubiquitination and degradation is repressed. A31N-ts20 cells were cultured in DMEM containing 10% FBS at 35°C in 90% air and 10% CO_2. When needed, cells were transferred to the restrictive temperature (39°C) 16 h before serum addition for inactivation of the thermosensitive E1 enzyme.

siRNA inhibition of NQO2 and NQO1 and stability of p53. Hep-G2 cells were seeded at a confluence of 70% before transfection. Predesigned control (scrambled sequences), NQO2 and NQO1 siRNA were purchased from Ambion. siRNA was transfected in different concentrations by HiPerFect transfection reagent (Qiagen) according to company's recommended protocol. At 48 h of post-transfection, the cells were lysed in radioimmunoprecipitation assay buffer [RIPA; 50 mmol/L Tris (pH 6.0), 150 mmol/L NaCl, 1% NP40, 5% deoxycholic acid, 0.1% SDS, 1 mmol/L phenylmethylsulfonyl fluoride (PMSF), and 1 mol/L Na-vanadate] supplemented with phosphatase inhibitor cocktail (Sigma) and protease inhibitors from Roche Diagnostics and analyzed by Western blotting using p53, NQO2, NQO1, and actin antibodies. Similar experiments were also done with A31N-ts20 cells. The cells were transfected at 35°C and incubated at ubiquitin-deficient restrictive temperature 39°C to study the effect of NQO2 and NQO1 siRNA on p53 degradation/stability.

p53-luciferase assay. Hep-G2 cells were cotransfected with 1 μg p53-Luc (14× enhancer element of p53, TGCCTGGACTTGCCTGG, containing luciferase reporting plasmid PathDetect *in vivo* signal transduction pathway *cis*-reporting systems, Stratagene), 50 ng pFC-p53 (Stratagene, containing full-length p53 cDNA under the control of a cytomegalovirus promoter) and control siRNA or NQO2 siRNA or NQO1 siRNA. An amount of 0.02 μg of Renilla luciferase was included in each case as control of transfection efficiency. Cells were collected after 24 h, lysed in RIPA, and analyzed for luciferase activity. Cells transfected with both pFC-p53 and p53-luc was used as 100%-fold change of luciferase activity to quantify the experiment.

Apoptosis assay. Hep-G2 cells were grown in monolayer in six-well plates and transfected with siNQO2 or siNQO1 RNA at increasing concentration using HiPerFect transfection kit. After 72 h of incubation, cells were used for flow cytometric analysis according to procedures as described (9). Cells were trypsinized and dispensed 1×10^5 per reaction in polypropiline tube and incubated with Annexin V antibody conjugated with FITC (BD PharMingen) on ice in the dark for 30 min. Cells were fixed and stained with propidium iodide, and apoptotic cells were counted as described by the manufacturer using a Coulter Epics XL-MCL flow cytometer. On the basis of Annexin V versus propidium iodide staining pattern, cells were sorted into nonapoptotic and apoptotic cells and percentage of apoptosis cells were tabulated.

Isolation of peritoneal macrophages and determination of the rate of degradation of NQO2, NQO1, and p53. Wild-type, NQO2-null, and NQO1-null mice were euthanized. The resident peritoneal exudate cells were collected from the mice by the previously described method (19). Briefly, 3 mL of sterile PBS was introduced in peritoneal cavity of euthanized mice and PE cells collected by gentle aspiration. The cells were washed by centrifugation at 400 × *g* for 10 min, and pellet was resuspended in DMEM containing 10% FCS supplemented with 10 mmol/L HEPES, 100 units/mL penicillin, and 100 μg/mL streptomycin. Differential cell counts were done on cytospin preparations stained with Wright Gimsa. More than 90% of the cell preparation were identified as macrophages by microscopic observation, and the macrophages were routinely found to be >95% viable by use of trypan blue exclusion. Cells were seeded in six-well plates (2×10^6 per well), allowed to settle overnight, and then treated with 10 μmol/L MG132 (Calbiochem) for 5 h in 10% FCS containing DMEM. The cells were washed and treated with cyclohexamide 30 μg/mL for different time periods. At the termination of experiment, the cells were washed twice with ice-cold PBS and processed for Western blotting.

Proteasome inhibition and stability of p53. Keratinocytes derived from tumors in wild-type, NQO2-null, and NQO1-null mice were grown in monolayer by procedure as previously described (20). The cells were treated with 5 μmol/L MG132 for 0 to 8 h or 50 μmol/L lactacystin (Sigma) for 6 h. Cells were lysed in ice-cold RIPA. Fifty micrograms of protein were loaded in each lane and separated on 12% SDS-PAGE, blotted on the enhanced chemiluminescence (Amersham; ECL) membranes and probed with antibodies against tumor suppressor proteins p53 (Novocastral Laboratories, Ltd.) and actin (Sigma).

BD Matchmaker mammalian assay. We used BD Matchmaker mammalian assay kit 2 and GreatEscAPe SEAP chemilumiescence detection kit from Clontech to determine direct interaction of NQO2 and NQO1 with p53. Full-length mouse NQO2 and NQO1 cDNA were separately cloned in plasmid VP16 to generate expression plasmids VP16mNQO2 and VP16mNQO1. Hepa-1 cells were grown in monolayer and cotransfected with various plasmids in the following combinations: pM+pVP16+pG5SEAP (control); pM-p53+pVP16+pG5SEAP (p53 control); pM+pVP16-mNQO2+pG5SEAP (NQO2 control); pM+pVP16-mNQO1+pG5SEAP (NQO1 control); pM-p53+pVP16-mNQO2+pG5SEAP (NQO2 interaction with p53); pM-p53+pVP16-mNQO1+pG5SEAP (NQO1 interaction with p53); pM3-VP16+pG5SEAP (positive control vectors encoding interacting proteins). The SEAP activity in culture supernatant was determined using a BD GreatEscAPe SEAP chemiluminescence detection kit according to the manufacturer's instructions.

***In vitro* 20S degradation of p53.** Full-length p53, NQO2, and NQO1 were *in vitro* transcribed and translated using [^{35}S]methionine and rabbit reticulocyte lysate from Promega by procedures as recommended by the manufacturer. Purified rabbit 20S proteasomes was purchased from Sigma. Two micrograms of *in vitro* translated p53 were mixed with similar amounts of bovine serum albumin, purified 20S proteasomes, *in vitro* translated NQO2 and NQO1, and 1 mmol/L NADH or 500 μmol/L NRH in different combinations in degradation buffer [100 mmol/L Tris-Cl (pH 7.5), containing 150 mmol/L NaCl, 5 mmol/L $MgCl_2$, and 2 mmol/L DTT] and incubated for 0 and 1 h at 37°C. All samples were mixed with Laemmli denaturation buffer, heated at 95°C for 5 min, and electrophoresed on 10% SDS-PAGE. The gel was dried and autoradiographed.

Preparation of mice liver cytosol and purification of 20S proteasome fractions. Livers from wild-type, NQO2-null, and NQO1-null mice were surgically removed, homogenized in buffer containing 20 mmol/L Tris-Cl (pH 7.5), 1 mmol/L EDTA, 1 mmol/L DTT, 1 mmol/L DMF, and 250 mmol/L sucrose. The cytosols were prepared by procedures as reported previously (7). To prepare 20S fractions, the cytosols were subjected to 38% to 70% ammonium sulfate precipitation and centrifugations. The precipitate was resuspended in buffer containing 20 mmol/L Tris-Cl (pH 7.5), 1 mmol/L DTT, 20% glycerol, 1 mmol/L PMSF, and loaded on a Sepharose 6B gel filtration column. Fractions of 0.5 mL were collected and analyzed for the presence of 20S proteasomes. The 20S-containing fractions were analyzed by SDS-PAGE and Western blotting to detect the presence of p53, NQO1, NQO2, 26S, and actin. The antibodies that probed the Western blots were rabbit polyclonal anti-20S proteasome core subunits (Calbiochem), rabbit polyclonal anti-p53 (NCL-p53-CM5P from Novocastral Laboratories), rabbit–anti-NOQ1 (laboratory generated), goat–anti-NQO2 (N-15 from Santa Cruz Biotechnology), rabbit–anti-26S proteasome, S6-subunit from Calibiochem, and mouse–antiaction from Sigma.

Immunoprecipation. About 200 μg to 1 mg of mice liver cytosols or 20S fractions or cell lysates were used for immunoprecipition. Briefly, cytosolic extract or 20S fraction was incubated with either rabbit IgG or anti-20S antibody for overnight at 4°C with shaking. The immunoprecipitation reaction was done in RIPA [50 mmol/L Tris (pH 6.0), 150 mmol/L NaCl, 1% NP40] containing 5% deoxycholic acid, 0.1% SDS, 1 mmol/L PMSF, and

1 mol/L Na-vanadate supplemented with phosphatase inhibitor cocktail and protease inhibitors. Washed Protein A beads (40 μL; Santa Cruz Biotechnology) were added, and the mixture was incubated for 1 h at 4°C with shaking. The slurry was centrifuged at 10,000 rpm 30 s, and supernatant was discarded. The beads were washed five times with RIPA. Residual buffer was sucked using fine tips up to dried condition. SDS-sample dye (50 μL) was added and boiled, and immunoprecipitates were resolved on a 10% SDS-PAGE followed by immunoblotting with indicated antibodies. Flag immunoprecipitation was done using the Flag-agarose beads (Sigma).

Purification of NQO1. NQO1 was purified from wild-type and NQO1-null mice keratinocytes by procedure as previously described (21). Five confluent (80–90%) 75-cm^2 flasks of wild-type and NQO1-null cells were lysed in RIPA lysis buffer. Dicumarol columns were equilibrated/washed with 5 mL RIPA. Cell lysates were added to the columns and allowed to decant by gravity at 4°C. The columns were then washed thrice with 5 mL RIPA containing protease inhibitors. NQO1 was eluted with 50 μmol/L NADH in RIPA buffer. Eluates, at 10, 20, and 40 μL, were resolved on 12% SDS polyacrylamide gels, blotted on the ECL membranes, and probed with antibodies against NQO1 and the tumor suppressor proteins p53. Western blots were developed with ECL reagents by the procedures suggested by the manufacturer.

Radiation and chemical exposure. A31N-ts20 cells were cultured at 35°C and either untransfected or transfected with HA-p53 and siNQO2, siNQO1, or control siRNA individually or in combination. The cells were incubated for 48 h at 35°C and then transferred to 39°C for 24 h. The cells were either unexposed or exposed to 4 Gy γ radiations and cultured at 39°C for another 4 h. The cells were lysed and analyzed by Western blotting and probing with anti-NQO2, anti-NQO1, anti-p53, and antiactin antibodies.

Keratinocytes from wild-type, NQO2-null, and NQO1-null mice were treated with 1,200 nmol benzo(*a*)pyrene in acetone. The control cells received acetone alone. The cells were harvested 24 h after the treatment, lysed, and analyzed by Western blotting and probing with NQO2, NQO1, p53, and actin antibodies.

Results

Inhibition and overexpression of NQO2 and NQO1 lead to alterations in levels of tumor suppressor p53. Previous studies

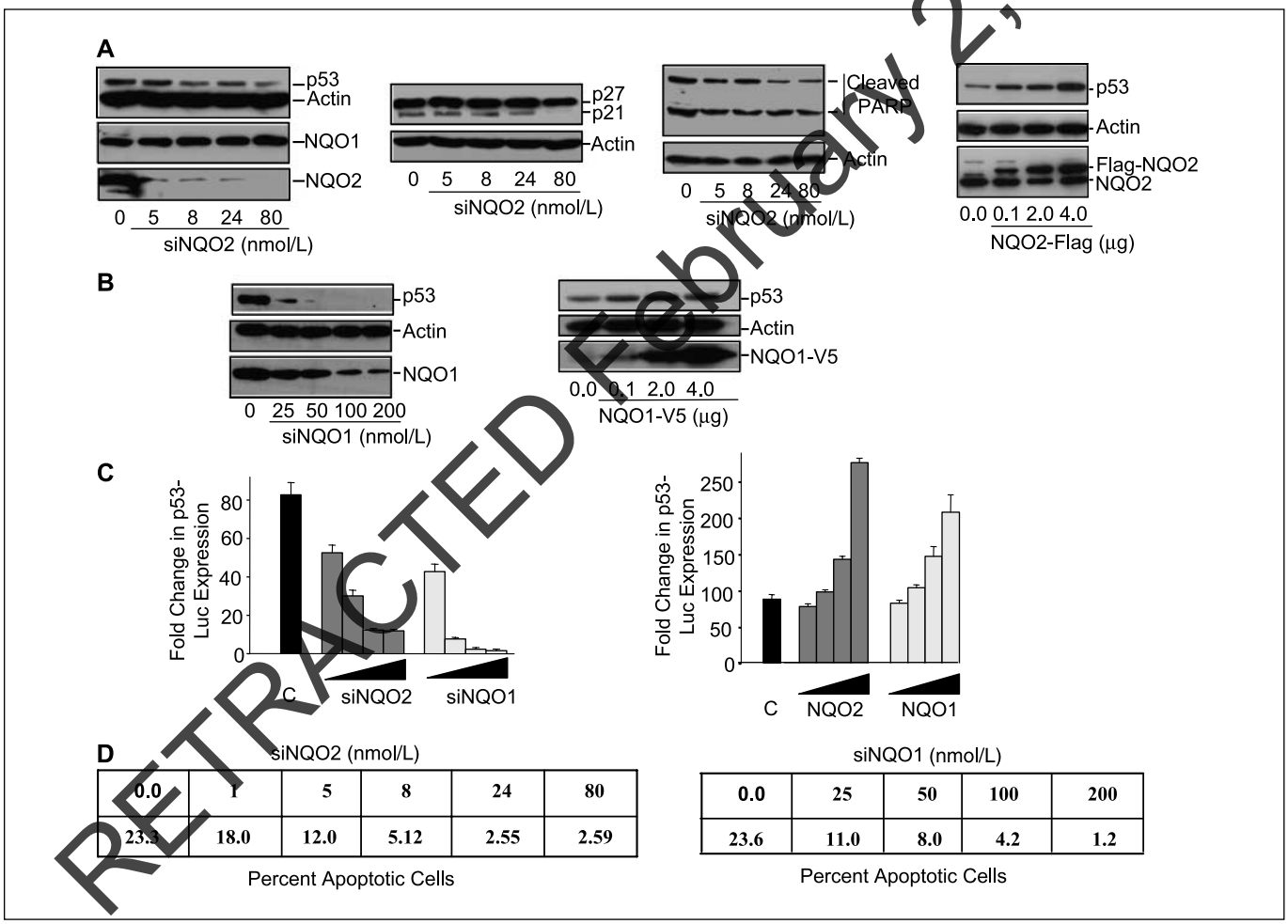

Figure 1. Inhibition or overexpression of NQO2 and NQO1 leads to alterations in stability of p53. *A,* Western analysis. Human hepatoblastoma Hep-G2 cells in left three panels were transfected with indicated amounts of siNQO2 RNA. The lane showing 0 siNQO2 was transfected with 80 nmol/L control scrambled siRNA. The Hep-G2 cells in right-most panel were transfected with increasing concentration of Flag-NQO2 expression plasmid. The lane showing 0.0 was transfected with 4.0 μg of control Flag vector. The transfected cells were lysed. The lysates were separated on SDS-PAGE, Western blotted and probed with NQO2, NQO1, p53, p27, p21, Flag, and actin antibodies. *B,* Western analysis. Hep-G2 cells were transfected with increasing concentrations of siNQO1 RNA (*left*) or pcDNA-NQO1-V5 plasmid (*right*). The cells were lysed, Western blotted, and probed with p53, NQO1, V5, and actin antibodies. *C,* p53-luciferase assay. *Left,* Hep-G2 cells were cotransfected with a fixed concentration of pFc-p53 expression, p53-luciferase (*p53-Luc*), and renilla luciferase plasmids and an increasing concentration of siNQO2 or siNQO1 RNA, lysed and analyzed for luciferase activity. The control lane (*C*) shows fold increase in p53-Luc expression in cells overexpressing p53 from pFc-p53 plasmid compared with vector transfected control. *Right,* Hep-G2 cells were cotransfected with increasing concentration of pcDNA-NQO2 or pcDNA-NQO1 expression plasmid and fixed concentrations of p53-luciferase and renilla luciferase, lysed and analyzed for luciferase activity. *D,* apoptotic cell death. Hep-G2 cells were transfected with indicated concentrations of NQO2 or NQO1 siRNA, incubated for 72 h, treated with Annexin V, and analyzed for apoptotic cells by flow cytometry.

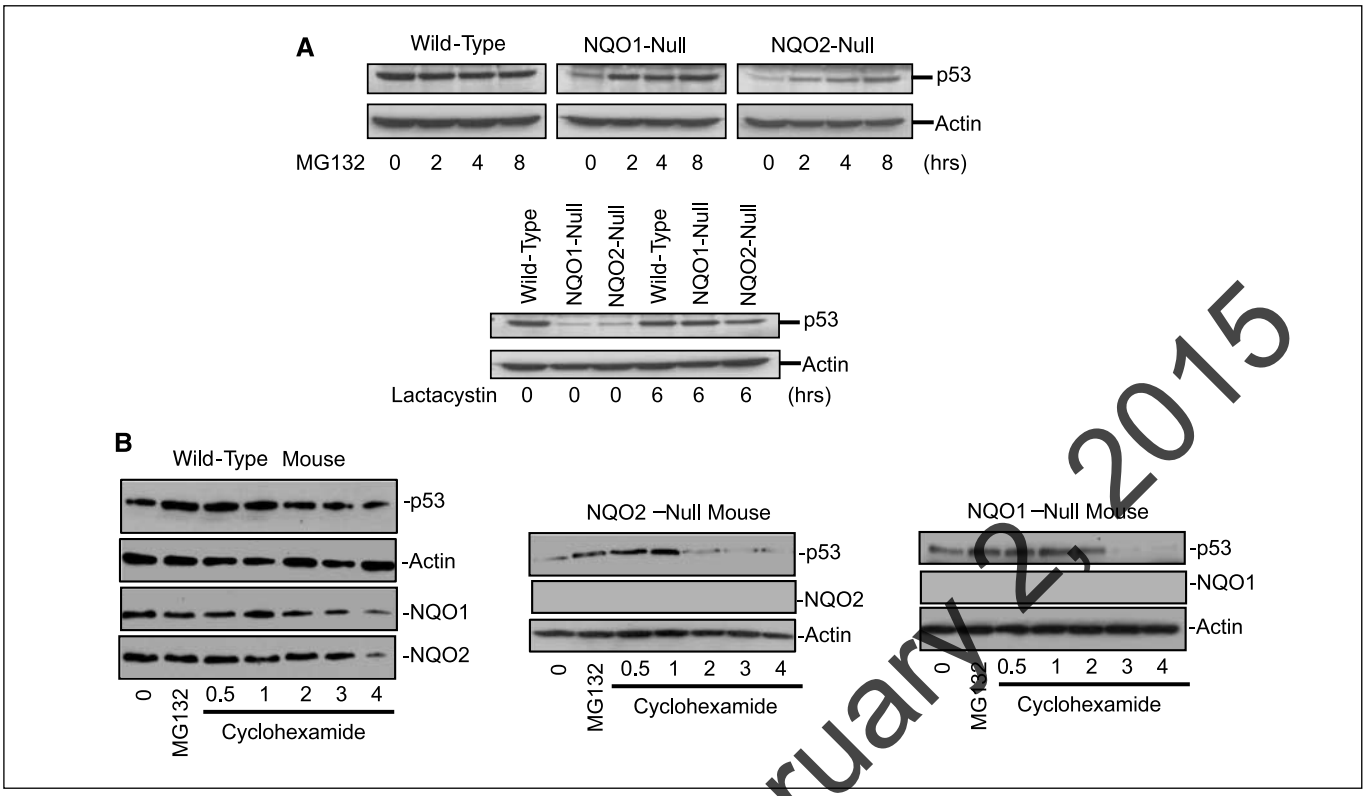

Figure 2. Proteasome inhibitors stabilize p53 in NQO2 and NQO1-null cells. *A,* degradation of p53 in wild-type, NQO2-null, and NQO1-null keratinocytes. Wild-type, NQO1-null, and NQO2-null keratinocytes were treated with 5 μmol/L MG132 for 0–8 h or 50 μmol/L lactacystin for 6 h. The concentrations and time used for MG132 and lactacystin treatments did not lead to cell death as determined by visual observations under the microscope and 3-(4,5-dimethylthiazol-2-yl)-2,5-diphenyltetrazolium bromide assay of viability test (data not shown). Cells were lysed in ice-cold RIPA. Fifty micrograms of protein were loaded in each lane and separated on SDS polyacrylamide gels, blotted on the ECL membranes, and probed with antibodies against tumor suppressor proteins p53 and actin. *B,* degradation of p53 in wild-type, NQO2-null, and NQO1-null mouse macrophages. Wild-type, NQO2-null, and NQO1-null mouse macrophages were treated with MG132 for 5 h, washed and treated with cycloheximide. The cells were collected at varying time intervals, lysed, and analyzed by Western blotting and probing with p53, NQO2, NQO1, and actin antibodies. The experiments in *B* were done thrice, and results were reproducible. Representative experiments.

in our laboratory showed lower basal levels and reduced induction of p53 in skin from NQO1-null and NQO2-null mice compared with wild-type mice (7, 10–13). These observations raised questions if inhibition or overexpression of NQO2 and NQO1 in human cells will also lead to similar alterations in levels of p53. The Hep-G2 cells were transfected with siRNA to inhibit NQO2, NQO1 and pCMV-Flag-NQO2, pcDNA-NQO1-V5 to over express NQO2 and NQO1 in separate experiments. Western blot analyzed the transfected cells for protein levels of NQO2, NQO1, p53, and p53 downstream gene products. The results are shown in Fig. 1. The cells transfected with NQO2 siRNA showed dose-dependent decrease in NQO2 and reduction in p53 and p53 downstream proteins p21 and p27 (Fig. 1*A, left two panels*). The decrease in NQO2 also showed dose-dependent suppression of PARP cleavage (Fig. 1*A, third panel from the left*). In addition, the transfection of Hep-G2 cells with pCMV-Flag-NQO2 led to dose dependent over expression of NQO2 and increase in p53. In similar experiments, NQO1 siRNA and pcDNA-NQO1-V5 showed dose-dependent decrease and increase in NQO1, respectively, and similar alterations in p53 (Fig. 1*B*). The NQO2 and NQO1 siRNA mediated decrease in p53 also led to decreased p53-luciferase gene expression and reduced spontaneous apoptosis in transfected Hep-G2 cells (Fig. 1*C, left,* and *D*). Similarly, over-expression of NQO2 and NQO1 led to increase in p53 and p53-luciferase gene expression (Fig. 1*C, right*). All these results showed that decrease or increase in NQO2 and NQO1 leads to respective decrease or increase in p53.

Loss of NQO2 and NQO1 leads to destabilization of p53. Next, we determined if the loss of p53 in NQO2-deficient and NQO1-deficient mice is because of the degradation of p53. Keratinocytes isolated from chemically induced skin tumors in wild-type, NQO2-null, and NQO1-null mice were treated with proteasome inhibitors MG132 and lactacystin in separate experiments for different time intervals (Fig. 2*A*). MG132 and lactacystin both inhibit proteasomes. MG132 inhibits the complex's chymotrypsin-like activity in a potent but reversible manner. Lactacystin is a natural, irreversible, nonpeptide, cell permeable inhibitor. Western blotting analyzed the p53 in keratinocytes treated with MG132 and lactacystin in separate experiments (Fig. 2*A*). Untreated NQO2-null and NQO1-null cells showed significantly lower expression of p53, compared with wild-type cells. This was expected because lower levels of p53 in NQO2-null and NQO1-null mice skin are reported (12, 13). Interestingly, the treatment with MG132 and lactacystin both stabilized p53 in NQO2-null and NQO1-null cells to the levels comparable with p53 in wild-type cells. These results indicated that lower p53 levels in skin of NQO2-null and NQO1-null mice are most likely due to rapid degradation of p53 in the absence of NQO2 and NQO1, respectively. In related experiments, macrophages were isolated from wild-type, NQO2-null, and NQO1-null mice treated with MG132 and cycloheximide and analyzed for the rate of degradation of endogenous p53 to confirm the results on degradation of p53 obtained from keratinocytes. The results from macrophages are shown in

Fig. 2*B*. The treatment of macrophages with proteasome inhibitor MG132 stabilized p53 in macrophages from all three genotypes. However, the rate of degradation of p53 differed among wild-type and null genotypes. The rate of degradation of p53 was significantly higher in macrophages from NQO2-null and NQO1-null mice, compared with macrophages from the wild-type mice (compare three panels of p53 in Fig. 2*B*). This was evident from the loss of most of p53 by 3 h in NQO2-null and NQO1-null cells, compared with little loss of p53 in wild-type cells. These results combined led to the conclusion that loss of NQO2 and NQO1 leads to rapid degradation of p53.

NQO2 and NQO1 interact with p53. The above results raised questions regarding how NQO2 and NQO1 protect p53 from degradation. Because NQO1 interaction with p53 was reported earlier (17), we tested the hypothesis that NQO2 and NQO1 directly interact with p53. We used immunoprecipitation, purification, and BD Bioscience matchmaker assays to study physical interaction of NQO2 and NQO1 with p53. The results are shown in Fig. 3. Hep-G2 cells were cotransfected with p53 and Flag-NQO2 plasmids, lysed, and analyzed for NQO2 and p53 interaction by immunoprecipitation with anti-Flag and Western analysis with anti-Flag and anti-p53 antibodies. The anti-Flag, but not IgG, immunoprecipitated Flag-NQO2 (Fig. 3*A*). p53 coprecipitated with Flag-NQO2 (Fig. 3*A*). This result indicated a direct interaction of NQO2 with p53. The Flag addition at the NH_2 terminus of NQO1 inactivated NQO1. Therefore, we used dicumarol column to purify endogenous cytosolic NQO1 from wild-type and NQO1-null keratinocytes. The NQO1 protein was successfully purified from wild-type, but not from NQO1-null, keratinocytes as expected (Fig. 2*B*). Interestingly, p53 copurified with NQO1. This suggested NQO1 interaction with p53. The NQO1 interaction with p53 has been reported earlier (16). The physical interaction between NQO2 and NQO1 with p53 was further confirmed by mammalian two-hybrid matchmaker assays (Fig. 3*C*). NQO2 interaction with p53 expressed significantly higher SEAP in the medium compared with NQO2 and p53 alone ($P < 0.0001$; Fig. 3*C*). Similar results were also observed for NQO1 and p53. All these results combined revealed that NQO2 and NQO1 physically interact with p53.

NQO2 and NQO1 coprecipitate and copurify with 20S proteasome. Next, we determined the role of 20S proteasomes in NQO2 and NQO1 protection of p53. 20S and 26S proteasome fractions were successfully purified from wild-type, NQO2-null, and NQO1-null mice livers (Fig. 4*A*, results shown only for 20S). Interestingly, p53, NQO2, and NQO1 all copurified with 20S but not with 26S proteasomes from wild-type liver cytosol (data shown only for 20S proteasomes). This indicated the involvement of 20S proteasome in NQO2 and NQO1 protection of p53. As expected, NQO2 did not copurify with 20S from NQO2-null mice and NQO1 did not copurify with 20S from NQO1-null mice. 20S proteasomes were successfully immunoprecipitated from purified 20S fractions and liver cytosols from wild-type, NQO2-null, and NQO1-null mice (Fig. 4*B* and *C*). Interestingly, p53 but not NQO2 or NQO1 coprecipitated with 20S proteasomes. These results revealed that 20S largely interacts with p53, but not with NQO2 and NQO1. In

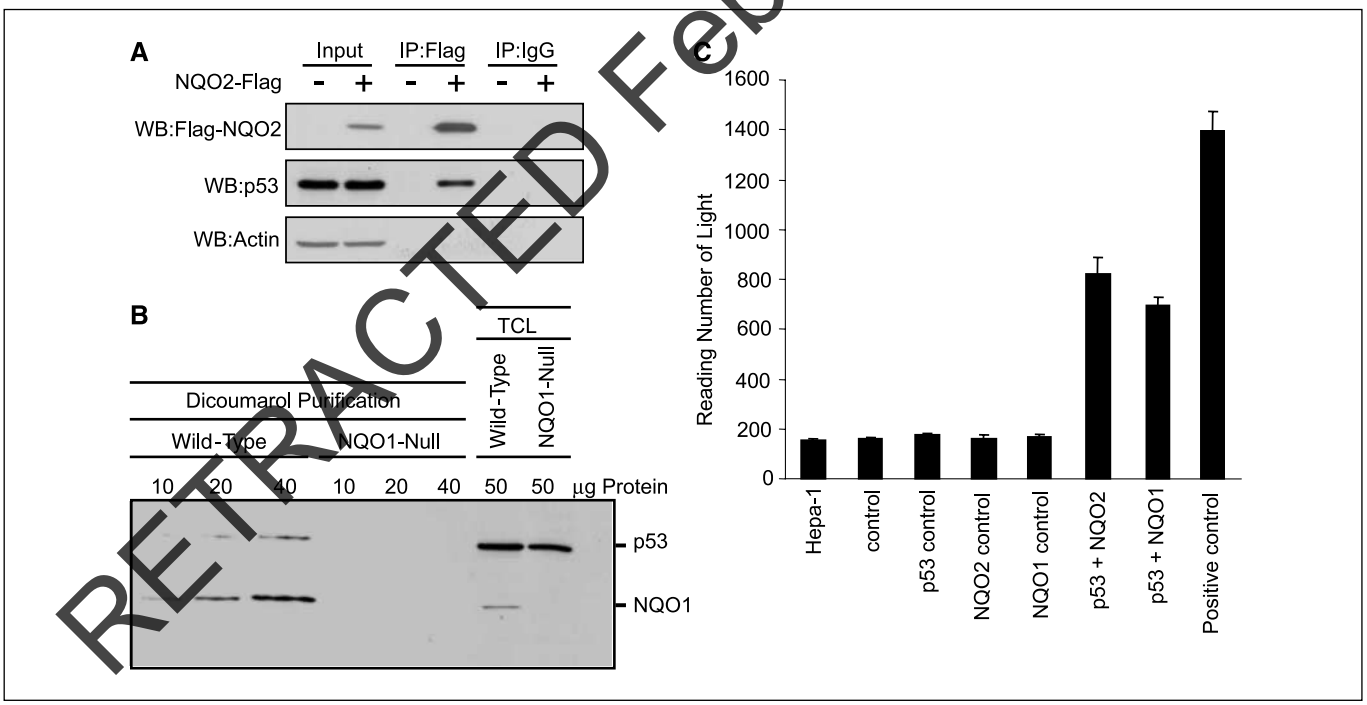

Figure 3. NQO2 and NQO1 interaction with p53. *A,* immunoprecipitation. Hep-G2 cells were transfected with Flag vector or Flag-NQO2 expression plasmid. The NQO2-Flag transfected cells were lysed and immunoprecipitated with anti-Flag and IgG antibodies and analyzed by Western blotting and probing with anti-Flag and anti-p53 antibodies. *B,* copurification of p53 with NQO1. Wild-type and NQO1-null keratinocytes were lysed with cold RIPA and protease inhibitor cocktail. Lysates were passed through dicumarol column. Columns were washed by passing excess amount of RIPA. NQO1 protein was then eluted, separated on polyacrylamide gels, blotted on the ECL membrane, and probed with antibodies against p53 and NQO1. The last two lanes were loaded with 50 μg of total cell lysate (*TCL*) of wild-type and NQO1-null keratinocyte cells. *C,* SEAP assay. Mouse hepatoma Hepa-1 cells were transfected with the plasmids in combinations: control (pM+pVP16+pG5SEAP); p53 control (pM-p53+pVP16+pG5SEAP); NQO1 control (pM+pVP16-mNQO1+pG5SEAP); NQO2 control (pM+pVP16-mNQO2+pG5SEAP); NQO2 interaction with p53 experiment (pM-p53+pVP16-mNQO2+pG5SEAP); NQO1 interaction with p53 experiment (pM-p53+pVP16-mNQO2+pG5SEAP); positive control (pM3-VP16+pG5SEAP, which have vectors encoding interacting proteins). The SEAP activity in culture supernatant was determined using a BD Great EscAPeTM SEAP chemiluminescence detection kit (Clontech) according to the manufacturer's instruction. *Columns,* mean of five independent experiments; *bars,* SD.

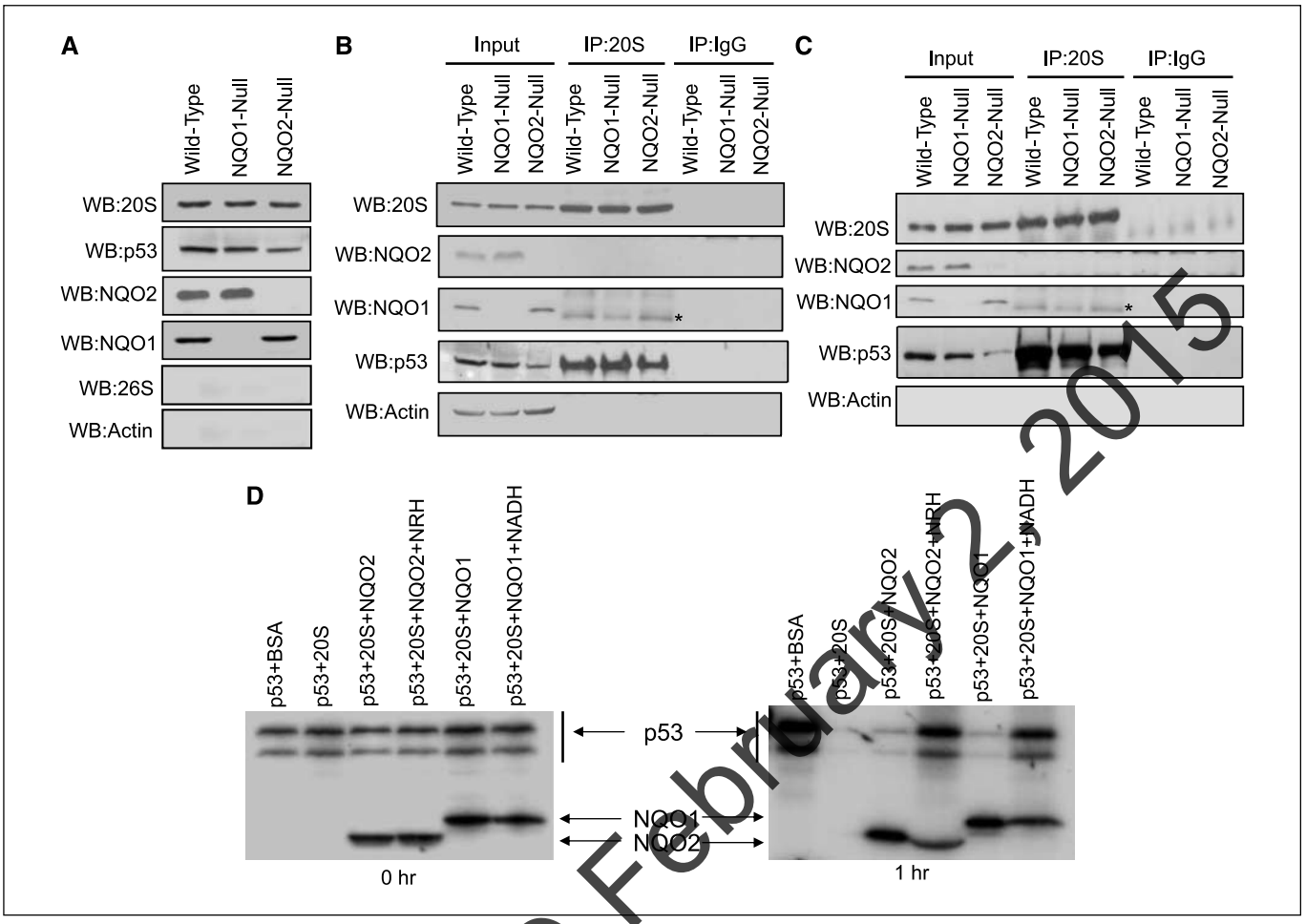

Figure 4. NQO2 and NQO1 interaction with p53 and protection against 20S proteasomal degradation of p53. *A,* Western analysis of purified 20S proteasomal fractions. NQO2, NQO1, and p53 copurify with 20S proteasomes. Livers from wild-type, NQO2-null, and NQO1-null mice were homogenized and subcellular fractionated. The 20S-containing fraction was purified and analyzed for the presence of p53, NQO1, NQO2, 26S, and actin. The proteins were separated on SDS-PAGE, Western blotted, and probed with rabbit polyclonal anti-20S proteasome core subunits, rabbit polyclonal anti-p53, rabbit–anti-NOQ1, goat–anti-NQO2, rabbit–anti-26S proteasome, S6-subunit, mouse–anti-actin antibodies. *B,* immunoprecipitation of liver 20S fractions. Two hundred micrograms of 20S proteasomes purified from livers of wild-type, NQO2-null, and NQO1-null mice were immunoprecipitated with rabbit–anti-20S antibody or rabbit–anti-IgG antibody. The proteins were separated on SDS-PAGE, Western blotted, and probed with 20S, NQO2, NQO1, p53, and actin antibodies. Input lanes contain one-tenth of the amount of 20S fraction used for immunoprecipitation. *C,* immunoprecipitation of liver cytosolic fractions. One milligram liver cytosolic proteins from wild-type, NQO1-null, and NQO2-null mice were immunoprecipitated with rabbit anti-20S antibody or rabbit–anti-IgG antibody. The proteins were separated on SDS-PAGE, Western blotted, and probed with 20S, NQO2, NQO1, p53, and actin antibodies. Input lanes contain one-tenth of the amount of cytosolic fractions used for immunoprecipitation. *D, in vitro* degradation of p53. NQO2 and NQO1 protection against 20S degradation of p53. *In vitro* reticulocyte lysate-translated [^{35}S]methionine-labeled p53 was incubated with 2 μg of purified 20S proteasome at 37°C for 1 h in the absence or presence of *in vitro* translated NQO2 or NQO1 together with or without 1 mmol/L NADH or 500 μmol/L NRH. Samples were mixed with Laemmli denaturation buffer, heated at 95°C for 5 min, and electrophoresed on SDS-PAGE. After electrophoresis, the gel was dried and exposed overnight at −70°C and autoradiographed. *, unspecific band.

other words, NQO1 and NQO2 copurify with 20S but do not interact with 20S.

NQO2 and NQO1 in the presence of their cofactor protect p53 from 20S proteasomal degradation. The above results raised the questions of the role of 20S in degradation of p53 and the role of NQO2 and NQO1 in protection of p53 from 20S-mediated degradation. We used *in vitro* translated p53, NQO2, and NQO1 proteins to study the role of NQO2 and NQO1 in protection of p53 from 20S degradation. Purified 20S proteasomes were purchased from Sigma. *In vitro* translated p53 was mixed with 20S in absence and presence of NQO2 and NQO1 and their cofactors and analyzed at 0 and 1 h after incubation. The results are shown in Fig. 4*D*. No degradation of p53 was observed at 0 h (Fig. 4*D, left*). Interestingly, 20S proteasomes degraded almost all of p53 in 1 h (Fig. 4*D, right*). The addition of NQO2 slightly protected the degradation of p53. However, inclusion of NQO2 and reduced cofactor NRH provided near total protection against 20S proteasomal degradation of p53. Similarly, NQO1 and its reduced cofactor NADH also provided significant protection against 20S proteasomal degradation of p53. These results led to the conclusion that NQO2 and NQO1, along with their reduced cofactor, protect p53 against 20S degradation.

NQO2 and NQO1 protect basal and radiation-induced p53 in ubiquitin-inactivated cells. We did experiments to determine that NQO2 and NQO1 protect p53 independent of ubiquitination of p53. In other words, 20S proteasome degradation does not require ubiquitination of p53. We also determined the role of NQO2 and NQO1 in protection of p53 in cells exposed to γ radiation. We used A31N-ts20, a BALB/c mouse cell line that harbors a temperature-sensitive E1 ubiquitin enzyme (18). The A31N-ts20 cells grown at

35°C are efficient in ubiquitination. These cells failed to show p53 in Western blot analysis because of ubiquitination and 26S proteasomal degradation of p53 (Fig. 5*A*). The incubation of A31N-ts20 cells at 39°C resulted in inactivation of ubiquitination and stabilization of p53. Exposure of cells to γ radiation led to increase in p53 in cells grown at a restrictive temperature of 39°C. We used siRNA to inhibit NQO2 and NQO1 and combined to determine the role of NQO2 and NQO1 in protection against ubiquitin-independent 20S proteasome degradation of p53. The NQO2 siRNA showed dose-dependent inhibition of NQO2 and increase in degradation of p53 in ubiquitin-deficient cells (Fig. 5*B, left radiation minus lanes*). Similar results were also observed with NQO1 siRNA (Fig. 5*B, middle radiation minus lanes*). NQO1 siRNA showed dose-dependent decrease in NQO1 and increase in degradation of p53. The exposure of cells to γ radiation–induced NQO2 and NQO1 that stabilized p53 (Fig. 5*B, left and middle*). The radiation increase in NQO1 was greater than NQO2. The overall effect on p53 stabilization was significant. The siRNA-mediated inhibition of NQO2 and NQO1 also resulted in increased degradation of p53 in cells exposed to γ radiation, as observed in cells unexposed to γ radiation. The control siRNA in the same experiment had no effect on degradation of p53 in radiation unexposed or exposed cells (Fig. 5*B, right*). In related experiment, the combined siRNA inhibition of NQO2 and NQO1 led to significant increase in degradation of p53, compared with inhibition by individual NQO2 and NQO1 proteins (Fig. 5*C*). These results combined revealed that NQO2 and NQO1 provide protection against ubiquitin-independent degradation of p53 by 20S proteasomes. The results also showed that radiation-induced expression of NQO2 and NQO1 led to stabilization of p53.

NQO2 and NQO1 protect basal and chemically induced p53 in keratinocytes. Next, we determined, if like radiation, environmental carcinogen benzo(*a*)pyrene induces NQO2 and NQO1 that leads to stabilization of p53. The keratinocytes isolated from tumors in wild-type, NQO2-null, and NQO1-null mice were exposed to benzo(*a*)pyrene, lysed, and Western blot–analyzed for NQO2, NQO1, p53, and control actin. The results showed that benzo(*a*)-pyrene induced expression of NQO2 and NQO1 that led

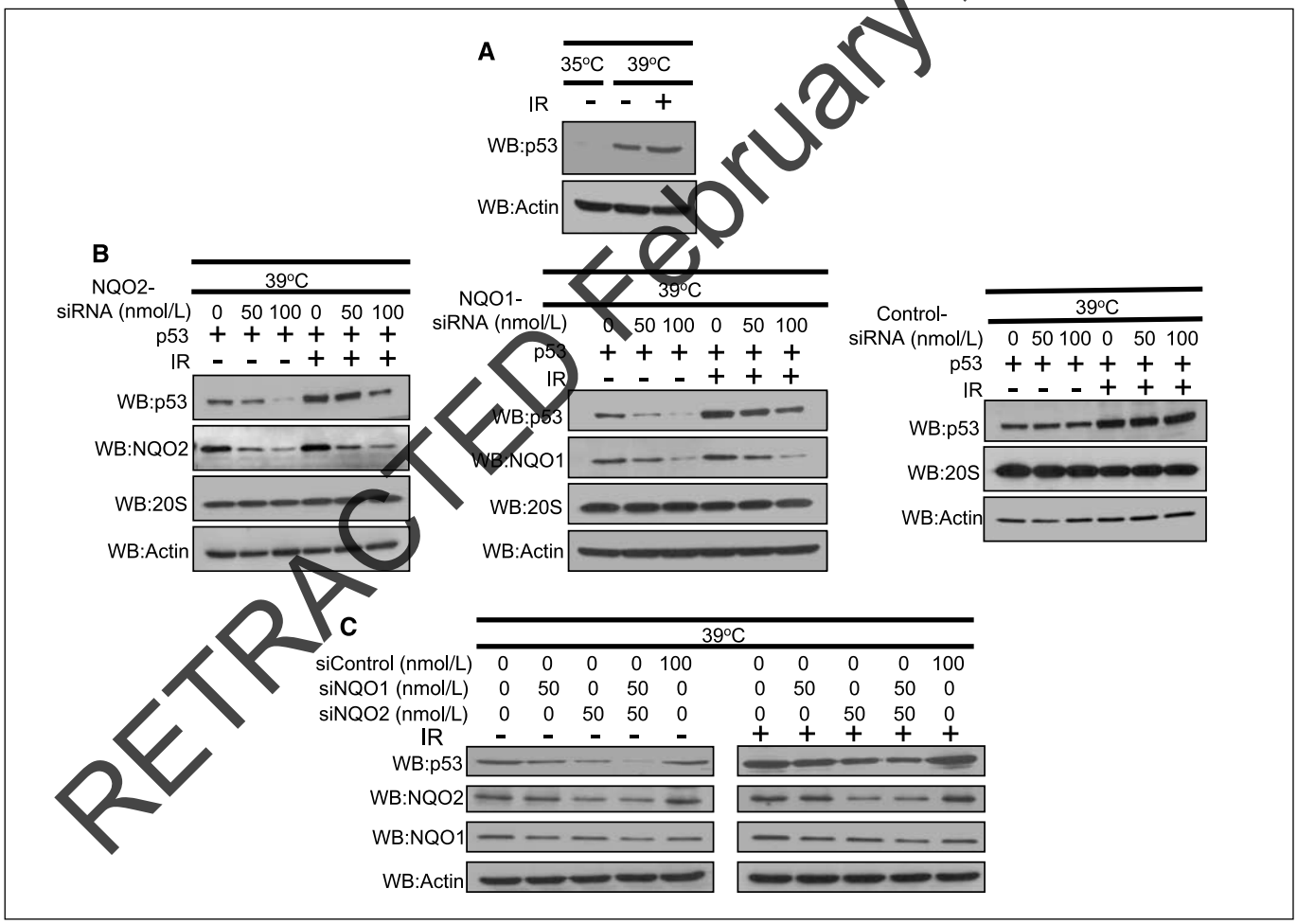

Figure 5. NQO2 and NQO1 protection against 20S proteasomal degradation of p53 in temperature-sensitive ubiquitin-deficient cells and effect of radiation. *A,* Western analysis. Expression of p53 in A31N-ts20 cells at permissive and restrictive temperatures. A31N-ts20 cells were cultured at 35°C (permissive temperature, ubiquitin positive) and 39°C (restrictive temperature, ubiquitin negative). The cells grown at 39°C were exposed to 4 Gy of γ radiation, lysed in RIPA, and analyzed by Western blotting and probing with anti-p53 and antiactin antibodies. *B,* siRNA transfection and Western analysis. A31N-ts20 cells were transiently transfected with HA-tagged p53 without and with increasing concentrations of NQO2-siRNA (*left*), NQO1-siRNA (*middle*), or control siRNA (*right*) at 35°C. The cells were incubated for 48 h at 35°C and then transferred to 39°C for 24 h. The cells were either unexposed or exposed to 4-Gy γ radiation, and cultured at 39°C for another 4 h. The cells were lysed and analyzed by Western blotting and probing with anti-NQO2, anti-NQO1, anti-p53, and antiactin antibodies. *C,* NQO2 and NQO1 siRNA combined transfection and Western analysis. NQO2 siRNA and NQO1 siRNA were combined in concentrations and experiments repeated as in *B*.

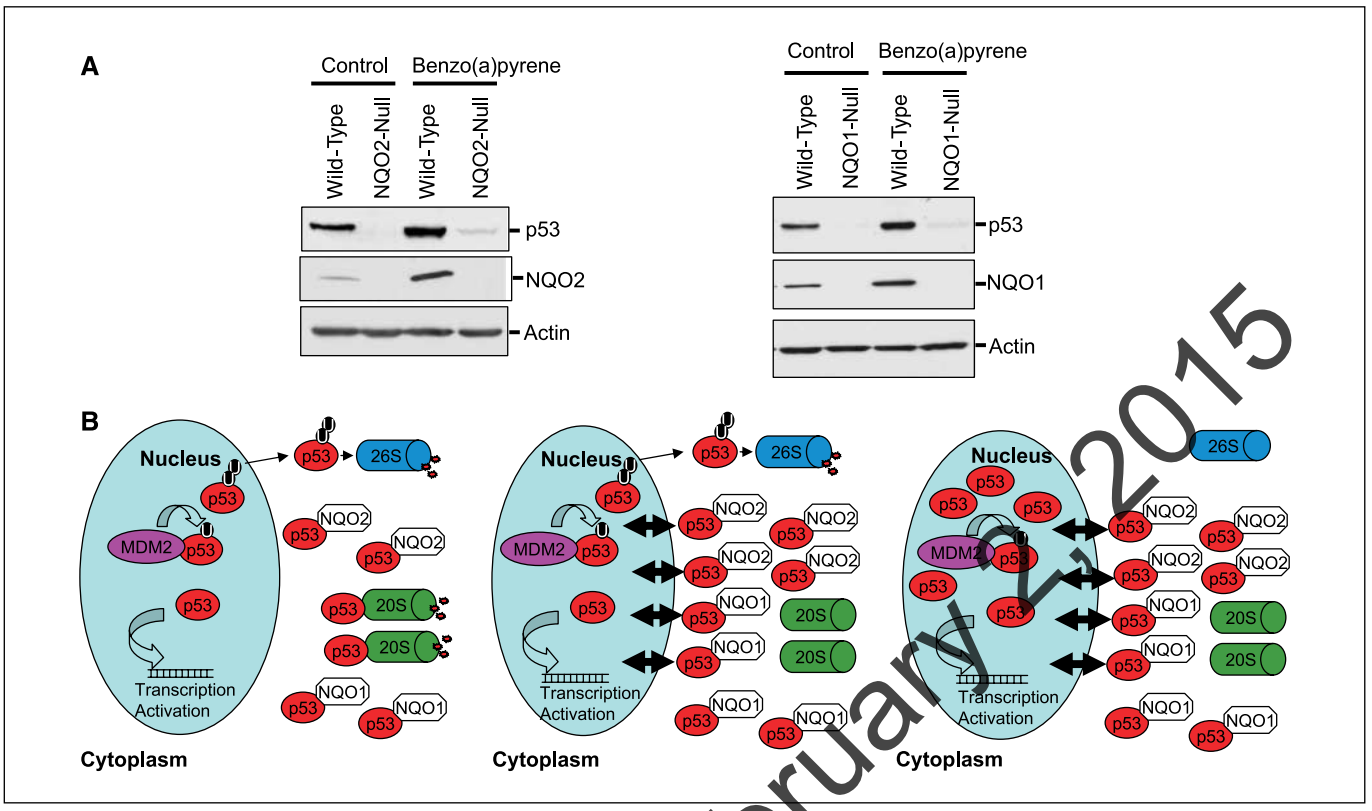

Figure 6. Chemical induction of NQO2 and NQO1 and protection against 20S degradation of p53. *A,* Western analysis. Benzo(*a*)pyrene induction of NQO2 and NQO1 and stability of p53. Wild-type and NQO2-null keratinocytes (*left*) and wild-type and NQO1-null keratinocytes (*right*) were treated with 1,200 nmol benzo(*a*)pyrene in acetone. Control cells received acetone alone. The cells were harvested and homogenized in appropriate buffer containing protease inhibitors. One hundred micrograms of homogenates were separated on SDS-PAGE, Western blotted, and probed with anti-NQO2, anti-NQO1, anti-p53, and antiactin antibodies. *B,* hypothetical model demonstrating the role of NQO1 and NQO2 in protection against 20S proteasomal degradation of p53.

to significant stabilization of p53 in wild-type cells (Fig. 6*A*). However, benzo(*a*)pyrene failed to cause significant stabilization of p53 in NQO2-null and NQO1-null cells (Fig. 6*A*).

Discussion

Tumor suppressor p53 plays an important role in protection of genome against internal and external stresses (22). It prevents cell transformation and tumor formation through transcriptional dependent and independent mechanisms (22). Therefore, the mechanisms that regulate synthesis, nuclear localization, and degradation of p53 are highly significant. Extensive studies that show the role of MDM2 in ubiquitination and 26S proteasome degradation of ubiquitinated p53 have been conducted (22). Chronic exposure of cells to radiation and chemicals leads to double strand breaks in DNA that leads to activation of ATM kinase (23). Activated ATM/ATR phosphorylates Chk1/2, MDM2, p53, and BRCA1 are the proteins that are involved in cell cycle arrest and DNA repair. Therefore, MDM2-p53 pathway is extensively studied and represents one of the major mechanisms of regulation of p53.

In this report, we present data that suggest a second interesting mechanism of the degradation and stabilization of p53. This mechanism is distinct from MDM2 and is independent of ubiquitination of p53. We showed that p53 is degraded by 20S proteasomes. 20S degradation of p53 is independent of ubiquitination, as this was also observed in ubiquitin-deficient cells. We also showed that cytosolic NQO2 and NQO1 protected 20S proteasomal degradation of p53. Overexpression of NQO2 and NQO1 stabilized p53 and decrease in NQO2 and NQO1 led to higher degradation of p53. This was evident from experiments in Hep-G2, A31N-ts20, and wild-type and null mouse models. The data on NQO1 stabilization of p53 are also supported by previous reports that suggested NQO1 stabilizes p53 (11). The data on NQO2 are presented for the first time in this report.

An intriguing question is how NQO2 and NQO1 protect p53? Several experiments, including immunoprecipitation, purification of NQO1, and BD Bioscience matchmaker assays, showed direct interaction of NQO2 and NQO1 with p53. The immunoprecipitation assays in the current studies clearly showed that NQO2 and NQO1 interact with p53 but not with 20S proteasomes. Therefore, it is possible that NQO2 and NQO1 interaction with p53 masks p53 interaction with 20S proteasomes. This leads to protection and stabilization of p53. The protein domains and the mechanism that regulate NQO2 and NQO1 interaction with p53 are unknown. It is reported earlier that the loss of NQO2 in NQO2-null mice and NQO1 in NQO1-null mice leads to lower p53 (12, 13). Similar results are observed with siRNA in transfected Hep-G2 cells in the present study. In other words, the NQO1 in NQO2-deficient and NQO2 in NQO1-deficient mice and cells failed to complement the loss of p53. It is possible that NQO1 and NQO2 heterodimerize or separately, but simultaneously, interact with p53 to protect p53 from 20S proteasomal degradation.

Our data suggest that acute exposure to radiation and chemicals induces NQO1 and NQO2, leading to stabilization of p53 in mice and cells expressing NQO1 and NQO2. However, the acute exposure of NQO1-deficient or NQO2-deficient mice, keratinocytes, or NQO1

and NQO2 siRNA transfected A31N-ts20 cells failed to increase p53. These results suggest that the induction of NQO1 and NQO2 might lead to transient activation of p53 that protects cells. Cellular induction of NQO1 and NQO2 in response to acute stresses including exposure to radiation, chemicals, drugs, metals, and environmental carcinogens are well documented (5). Induction of NQO1 and NQO2 is also known to protect against benzo(*a*)pyrene-induced and dimethylbenzanthracene-induced skin carcinogenesis in mice (11–13). This protection is presumably due to transient activation of p53 and increased metabolic detoxification of chemicals (12, 13). Therefore, it makes sense that NQO1 and NQO2 mediated transient activation/stabilization of p53 is required to deal with acute exposure of radiation and chemical stress.

A hypothetical model is shown in Fig. 6*B* to show the significance of NQO1 and NQO2 protection of p53 from 20S proteasomal degradation. In a normal cell, the nonubiquitinated p53 is degraded by 20S proteasomes and MDM2 ubiquitinated p53 is degraded by 26S proteasomes (Fig. 6*B, left*). A low level of p53 is maintained within the cell through interaction with NQO1 and NQO2. The acute exposure to radiation or chemical leads to increase in expression of NQO1 and NQO2 and stabilization of p53 because more of p53 is engaged by increased NQO1 and NQO2. The p53 degradation by 20S proteasomes is suppressed during acute exposure to radiation and chemicals (Fig. 6*B, middle*). During acute exposure, MDM2 pathway of p53 presumably remains unaffected. The NQO1 and NQO2 pathway seems to be important for day-to-day exposure to radiation and chemical through environment and intake of food and drugs. This pathway only transiently activates p53 through stabilization. The p53 levels presumably are brought back to normal levels once the stress effect disappears and NQO1 and NQO2 levels are normalized. Therefore, NQO1-mediated and NQO2-mediated stabilization of p53 promotes cell protection. The chronic exposure of cells to radiation or chemical also leads to inactivation of MDM2 and shutting of 26S proteasomal degradation of p53. Therefore, both 20S and 26S proteasomal degradation of p53 are suppressed (Fig. 6*B, right*). This leads to higher accumulation of p53 and most likely apoptotic cell death.

In conclusion, we present here data that show a role of NQO1 and NQO2 in protection against 20S degradation of p53. This leads to stabilization of p53 and cellular protection.

Acknowledgments

Received 1/25/2007; revised 3/12/2007; accepted 3/19/2007.

Grant support: NIH grant RO1 ES07948.

The costs of publication of this article were defrayed in part by the payment of page charges. This article must therefore be hereby marked *advertisement* in accordance with 18 U.S.C. Section 1734 solely to indicate this fact.

We thank Dr. Dorothy Lewis, Baylor College of Medicine, Houston, TX, for help in the flow cytometric analysis.

References

1. Pietsch EC, Humbey O, Murphy ME. Polymorphisms in the p53 pathway. Oncogene 2006;25:1602–11.
2. Dai M, Jin Y, Gallegos JR, et al. Balance of yin and yang: Ubiquitylation-mediated regulation of p53 and c-Myc. Neoplasia 2006;8:630–44.
3. Ross D, Kepa JK, Winski SL, et al. NAD(P)H:quinone oxidoreductase1 (NQO1): chemoprotection, bioactivation, gene regulation and genetic polymorphism. Chem Biol Interact 2000;129:77–97.
4. Long DJ II, Jaiswal AK. NRH:quinone oxidoreductase2 (NQO2). Chem Biol Interact 2000;129:99–112.
5. Jaiswal AK. Nrf2 signaling in coordinated activation of antioxidant gene expression. Free Radic Biol Med 2004; 36:1199–207.
6. Radjendirane V, Joseph P, Lee H, et al. Disruption of the DT diaphorase (NQO1) gene in mice leads to increased menadione toxicity. J Biol Chem 1998;273:7382–9.
7. Long DJ, Iskander K, Gaikwad A, et al. Disruption of dihydronicotinamide riboside:quinone oxidoreductase 2 (NQO2) leads to myeloid hyperplasia of bone marrow and decreased sensitivity to menadione toxicity. J Biol Chem 2002;277:46131–9.
8. Gaikwad A, Long DJ II, Stringer JL, et al. *In vivo* role of NAD(P)H:quinone oxidoreductase 1 (NQO1) in the regulation of intracellular redox state and accumulation of abdominal adipose tissue. J Biol Chem 2001;276: 22559–64.
9. Long DJ II, Gaikwad A, Multani A, et al. Disruption of the NAD(P)H:quinone oxidoreductase 1 (NQO1) gene in mice causes myelogenous hyperplasia. Cancer Res 2002; 62:3030–6.
10. Long DJ II, Waikel RL, Wang XJ, et al. NAD(P)H:quinone oxidoreductase 1 deficiency increases susceptibility to benzo(*a*)pyrene-induced mouse skin carcinogenesis. Cancer Res 2000;60:5913–5.
11. Long DJ II, Waikel RL, Wang XJ, et al. NAD(P)H:quinone oxidoreductase 1 deficiency and increased susceptibility to 7,12-dimethylbenz[a]-anthracene-induced carcinogenesis in mouse skin. J Natl Cancer Inst 2001;93: 1166–70.
12. Iskander K, Paquet M, Brayton C, et al. Deficiency of NRH:quinone oxidoreductase 2 increases susceptibility to 7,12-dimethybenz(a)anthracene and benzo(*a*)pyrene-induced skin carcinogenesis. Cancer Res 2004;64:5925–8.
13. Iskander K, Gaikwad A, Paquet M, et al. Lower induction of p53 and decreased apoptosis in NQO1-null mice leads to increased sensitivity of chemical-induced carcinogenesis. Cancer Res 2005;65:2054–8.
14. Asher G, Loten J, Cohen B, et al. Regulation of p53 stability and p53-dependent apoptosis by NADH quinone oxidoreductase 1. Proc Natl Acad Sci U S A 2001; 98:1188–93.
15. Asher G, Loten J, Kama R, et al. NQO1 stabilizes p53 through a distinct pathway. Proc Natl Acad Sci U S A 2002;99:3099–104.
16. Asher G, Loten J, Sachs L, et al. Mdm-2 and ubiquitin-independent p53 proteasomal degradation regulated by NQO1. Proc Natl Acad Sci U S A 2002;99:13125–30.
17. Anwar A, Dehn D, Siegel D, et al. Interaction of human NAD(P)H:quinone oxidoreductase 1 (NQO1) with the tumor suppressor protein p53 in cells and cell-free systems. J Biol Chem 2003;278:10368–73.
18. Salvat C, Acquaviva C, Scheffner M, et al. Molecular characterization of the thermosensitive E1 ubiquitin-activating enzyme cell mutant A31N-ts20. Eur J Biochem 2000;267:3712–22.
19. Kole L, Sarkar K, Mahato SB, et al. Neoglcoprotein-conjugated liposomes as macrophage-specific drug carrier in the therapy of leishmaniasis. Biochem Biophys Res Commun 1994;200:351–8.
20. Ahn KS, Sethi G, Jain AK, et al. Genetic deletion of NAD(P)H:quinone oxidoreductase 1 abrogates activation of nuclear factor-kB, IkBa kinase, c-Jun N-terminal kinase, akt, p38, and p44/42 mitogen-activated protein kinases and potentiates apoptosis. J Biol Chem 2006;281: 19798–806.
21. Segura-Aguilar J, Kaiser R, Lind C. Separation and characterization of isoforms of DT-diaphorase from rat liver cytosol. Biochim Biophys Acta 1992;1120:33–42.
22. Sun Yi. p53 and its downstream proteins as molecular targets of cancer. Mol Carcinog 2006;45: 409–15.
23. Lee MH, Lozano G. Regulation of the p53–2 pathway by 14–3-3 o˙ and other proteins. Semin Cancer Biol 2006; 16:225–34.

Cancer Research

Retraction: NRH:Quinone Oxidoreductase 2 and NAD(P)H:Quinone Oxidoreductase 1 Protect Tumor Suppressor p53 against 20S Proteasomal Degradation Leading to Stabilization and Activation of p53

The authors wish to retract the article titled "NRH:Quinone Oxidoreductase 2 and NAD(P)H:Quinone Oxidoreductase 1 Protect Tumor Suppressor p53 against 20S Proteasomal Degradation Leading to Stabilization and Activation of p53," which was published in the June 1, 2007, issue of *Cancer Research* (1). As a result of an error, the p53 and NQO2 panels in Fig. 6A were reused from Fig. 3B of the article titled "Lower induction of p53 and decreased apoptosis in *NQO1*-null mice lead to increased sensitivity to chemical-induced skin carcinogenesis" by Iskander and colleagues (2).

Two of the four authors agreed to this Retraction. Attempts on the part of the journal office to contact Xing Gong and Labanyamoy Kole were unsuccessful.

Karim Iskander
Onyx Pharmaceuticals, Inc., Houston, Texas

Anil K. Jaiswal
Department of Pharmacology, University of Maryland School of Medicine, Baltimore, Maryland.

References

1. Gong X, Kole L, Iskander K, Jaiswal AK. NRH:quinone oxidoreductase 2 and NAD(P)H:quinone oxidoreductase 1 protect tumor suppressor p53 against 20S proteasomal degradation leading to stabilization and activation of p53. Cancer Res 2007;67:5380–8.
2. Iskander K, Gaikwad A, Paquet M, Long DJ II, Brayton C, Barrios R, et al. Lower induction of p53 and decreased apoptosis in NQO1-null mice lead to increased sensitivity to chemical-induced skin carcinogenesis. Cancer Res 2005;65:2054–8.

Published online February 2, 2015.
doi: 10.1158/0008-5472.CAN-14-3458

NRH:Quinone Oxidoreductase 2 and NAD(P)H:Quinone Oxidoreductase 1 Protect Tumor Suppressor p53 against 20S Proteasomal Degradation Leading to Stabilization and Activation of p53

Xing Gong, Labanyamoy Kole, Karim Iskander, et al.

Cancer Res 2007;67:5380-5388.